Ultra Low-Noise Preamplifier for Low-Frequency Noise Measurements in Electron Devices

Bruno Neri, Bruno Pellegrini, and Roberto Saletti

Abstract—**The design and realization of an ultra low-noise high-input impedance amplifier for low-frequency noise measurements in electronic devices is presented. Special care is devoted to the solution of typical problems encountered in the design of low-noise low-frequency equipment, such as power supply noise and temperature fluctuations. The preamplifier has a bandwidth of over 7 decades with a low-frequency roll-off of 4 mHz. The noise characteristics obtained are sensibly better than those of commercial preamplifiers commonly adopted in low-frequency noise measurements. The application of this preamplifier to the realization of standard $1/f^{\gamma}$ noise generators is also presented.**

I. Introduction

NOISE is a disturbance in measurements and establishes the low limit which the observed quantity has to exceed, in order to obtain the required accuracy in the measurement itself. Also, noise is the measurable effect of several physical phenomena occurring in the sample under test (and in the measurement system, too) and thus carries much information about them. Because of this property, noise can be a very sensitive tool in the characterization of electronic devices, particularly in reliability and diagnostic fields [1a-e]-[5].

The most critical part of a low-frequency low-noise measurement system is the preamplifier, which usually establishes the sensitivity of the entire system. Commercial preamplifiers exhibit quite good performance in the frequency range above a few hertz, but the power spectral density of their equivalent input noise generator S_v sharply increases when frequency tends to zero with the well-known relationship

$$S_v \propto 1/f^{\gamma} \tag{1}$$

where f is the frequency and γ is usually greater than 1.

Moreover, commercial preamplifiers do not often allow the investigation of phenomena characterized by time constants of several seconds or more, because their low-frequency limit f_L is rarely less than 100 mHz. This sometimes represents an unacceptable limitation in the use of low-frequency noise measurements (LFNM) as a characterization technique. In fact, flicker noise can be used to perform defect spectroscopy of solid state devices [6], [7], and its existence has been experimentally proved at frequencies as low as 10^{-6} Hz [8].

Finally, new technological processes for electronic device fabrication make available materials characterized by a very low defectivity and, consequently, devices exhibiting always lower excess noise levels, sometimes comparable or even negligible with respect to the background noise of a commercial preamplifier itself. For instance, materials such as the metals generate an amount of excess noise typically well below the level measurable with the instrumentation available on the market. A conclusion of a paper published in 1975 was "... that, even within the highest achievable sensitivities, no detection is possible of any excess noise in metal conductors within the limits of sample volume and current density which can be obtained before the specimen destruction" [2].

The situation has not changed in last years because no remarkable improvements have been made to the low-frequency low-noise commercial preamplifiers most commonly used in research laboratories (for instance PAR 113 from Princeton Applied Research or Brookdeal 5003 from EG&G), whereas the LFNM technique is more and more used, especially in the characterization of VLSI thin metal film interconnections [3]-[5].

Therefore, researchers in the field of low-frequency noise measurement need custom amplifiers with improved noise performance, operating in a frequency band from millihertz to hundreds of kilohertz, characterized also by a sufficiently high input impedance and possibly by a low cost. Some custom low-noise amplifiers are proposed in the literature [9], [10], but none of them deals with or is suitable for application in the very low-frequency range.

In fact, some major problems are encountered in the design of an ultra low-noise preamplifier (ULNA) with a gain of at least 60 dB at frequencies as low as a few mHz.

The first is the power supply system, which can introduce undesired noise in the frequency range below 1 Hz. A value of f_L of some mHz leads to high values of the coupling capacitors. Because of their large dimensions, they introduce parasitic capacitive coupling between the input and the output of the preamplifier, making possible the onset of instabilities. Another critical point is the temperature fluctuation of the input active device, which can definitely impair performance at low frequency.

The aim of this paper is to describe design and realization of a low-cost ULNA characterized by a high input impedance, a low-frequency limit f_L of a few mHz and by a noise performance better than that of commercial preamplifiers, particularly below 10 Hz. This amplifier has been widely used and tested in our laboratory during the last 4 years in experimental measurements on noise in electronic devices.

II. Preamplifier Design

The circuit diagram of the ULNA described in this paper is quite simple and is reported in Fig. 1(a). It consists of two cascaded voltage-series feedback amplifiers of the type of Fig. 1(b), each one providing a gain of 34 and 46 dB, respectively, so that the total gain of the preamplifier is 80 dB.

Manuscript received February 20, 1990; revised September 26, 1990.

B. Neri and B. Pellegrini are with Istituto di Elettronica e Telecomunicazioni, University of Pisa, 56126 Pisa, Italy.

R. Saletti is with Centro di Studio per Metodi e Dispositivi per Radiotrasmissioni, Consiglio Nazionale delle Ricerche, 56126 Pisa, Italy.

IEEE Log Number 9041025.

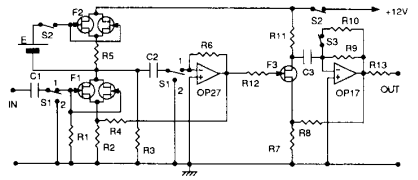

(a)

R_1=100 MΩ	R_{10}=750 kΩ
R_2=10 Ω	R_{11}=5.5 kΩ
R_3=1 kΩ	R_{12}=10 kΩ
R_4=500 Ω	R_{13}=500 Ω
R_5=165 Ω	
R_6=30 kΩ	C_1=9.4 μF
R_7=100 Ω	C_2=2200 μF
R_8=22 kΩ	C_3=220 μF
R_9=1.5 MΩ	E=2 V
F1, F2=Toshiba 2SK146	
F3=Toshiba 2SK147	
OP27=PMI OP27	
OP17=PMI OP17	

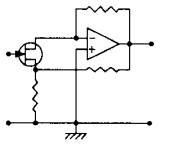

(b)

Fig. 1. Circuit diagram of the ultra low-noise amplifier described in the text (a), and reduced circuit of its two stages (b).

The input device $F1$ is a paralleled FET matched pair produced by Toshiba (2SK146). The equivalent input noise power spectral density S_f of one transistor of the pair shows a plateau of 0.7 $nV/(Hz)^{1/2}$ above 10 Hz, and a noise corner frequency f_c of about 3 Hz. Below f_c, S_f shows the flicker-like behavior of (1), where the frequency exponent γ assumes a value of 1.6–1.7 down to the lowest investigated frequency of 3 mHz. Similar noise characteristics can also be found in other low-noise transistors produced by Toshiba, such as 2SK369 and 2SK371.

Using a paralleled pair of input devices the value of S_f is reduced of a factor of 2, whereas the power spectral density of the input current noise generator S_i, as well as the input capacitance, are increased by the same factor [11]. It will be shown later that the resulting low value of S_i and its frequency dependence make this configuration very effective, whichever the source resistance is, below some kHz, that is in the most interesting frequency range for LFNM technique applications.

The dc value of the drain current I_D (10 mA) is imposed by the source resistance R_2 and represents a good compromise between a reduced power consumption and a low value of S_f.

In order to reduce the effects of thermal fluctuations, the input transistors are enclosed in a thermal filter constituted of a massive copper cylinder (diameter = 3 cm, height = 4 cm), which in turn is contained in a cork cylinder (diameter = 5 cm, height = 6 cm). A cutoff frequency relevant to the external thermal fluctuations of some tens of μHz, and thus a noticeable improvement in thermal fluctuation immunity is obtained, because of the high values of the copper thermal capacitance and the cork thermal resistance.

The input transistor pair $F1$ is loaded by the resistor R_3, whereas FET pair $F2$ is a current generator which supplies the current needed to bias $F1$. In this way, fluctuations originated in the power supply produce only negligible effects on the drain of $F1$. The battery E does not supply current and permits a high value of the bias resistor R_5, as compared to R_2, and thus a strong reduction in the gain of $F2$. Therefore, its equivalent input noise voltage generator produces a negligible effect on the drain of $F1$.

As far as the input high-pass filter (R_1–C_1) design is concerned, the value of R_1 determines the amplifier input resistance R_{in}, whereas the value of C_1 is chosen high enough so that the Johnson noise of R_1 is shunted and made negligible, with respect to S_f, in the amplifier bandwidth. This typically leads to a value of C_1 about one order of magnitude higher than that sufficient for the required low-frequency limit. For instance, a capacitor C_1 = 0.4 μF with R_1 = 100 MΩ would be sufficient for a roll-off frequency of 4 mHz, but the filtered thermal noise of R_1 would be greater than the FET noise. Thus, the value of the capacitor has to be increased up to 9.4 μF. In this case, the resulting input time constant is equal to 940 s and the charge of C_1 at the dc voltage of the signal source takes about 1 h. In order to avoid such a long settling time, a fast recovery can be performed by switching the switches S_1 to position 2 for about 1 min before any measurement. Because the feedback loop is broken, this action also causes the quick charging of C_2 to the drain voltage of $F1$.

In order to obtain a reliable gain and a high input impedance Z_{in} in the upper range of the bandwidth, a voltage series feedback loop is achieved by using a low-noise operational amplifier (OP27 produced by PMI), as reported in Fig. 1(a)–(b). The virtual ground of the OP27 inverting input allows one to consider the gate-drain capacitance C_{gd} of $F1$ in parallel with R_1, without the undesired magnifying factor due to the gate-drain Miller effect. The gate-source capacitance C_{gs} does not contribute to the input impedance in the preamplifier bandwidth, because the series feedback keeps a very low gate-source voltage in this frequency range. Therefore, the theoretical value of the input capacitance C_{in} is equal to C_{gd}. This statement and the amplifier design have been fully verified by means of a computer electrical simulation. Finally, the coupling capacitance C_2 is chosen so that a 2.8-mHz pole-frequency is obtained, whereas the resistor R_4 is 50 times R_2, in order to achieve the required first-stage gain of 34 dB.

The only remarkable difference in the second stage is a different operational amplifier: an OP17 produced by PMI. This device is a FET-input low-noise amplifier characterized by a low value of the input bias currents, which are the main components responsible for the preamplifier output offset voltage V_o. The maximum calculated V_o is about 2 mV. This value is well below the minimum amplitude range of digital signal analyzers usually adopted in noise measurements. Therefore, a circuitry for dc offset elimination is not necessary. The second stage input transistor $F3$ is a single 2SK147 FET (identical to one transistor of the 2SK146 pair). The parallel configuration required for noise optimization is needed no more, because the input signal level is amplified by 34 dB by the first stage. Furthermore, this solution allows a reduction in power consumption.

The power supply system is very important in this application because it has to generate a very low amount of noise. Rechargeable lead/acid batteries are used to supply the preamplifier. It was shown that noise generated by lead/acid batteries strongly depends on the ratio Θ between the supplied current and the battery nominal capacity [12]. For instance, a good choice is to maintain Θ less than 0.01 h^{-1}. This is obtained having employed lead/acid batteries with a capacity of 10.5 A · h.

Another problem to deal with is the stability of the system. It could seem trivial to make the system stable, for instance, by compensating the overall open loop gain of the network. On the contrary, this is a very hard step due to the high gain-bandwidth product (2 GHz) of the preamplifier and to the unevaluable and cabling-dependent stray capacitive couplings between the various components of the circuit. This is particularly true for the large-dimension capacitors C_1 and C_2 which constitute a major problem from this point of view. A reliable solution was obtained by dividing the shielding copper box which encloses the

preamplifier in five electrically shielded smaller boxes. Each one contains the input capacitor, the first stage, the second stage, a radiofrequency output filter (optional), and the supply batteries, respectively.

The radiofrequency output filter is an optional circuitry which is not reported in the schematic of Fig. 1. It is a simple low-pass R–C filter useful to prevent external electromagnetic interferences coupled through the output cable. In fact, radiofrequency signals can enter into the system, be revealed, and transformed in a low-frequency voltage fluctuation across a p-n junction acting as a rectifier, or across other devices with a nonlinear characteristic [12].

The low-frequency limit f_L can be changed by the switch S3 reported in Fig. 1 from 4 mHz (S3 open) to 8 mHz (S3 closed), without changing the dc voltage across C_3. The change in the total gain is about 0.3 dB and it is therefore acceptable to consider it constant and equal to 80 dB.

In order to minimize their flicker noise contribution, only metal-film resistors have to be used. In our ULNA we employ excess noise free resistors produced by Vishay.

III. Experimental Characterization

Several measurements were performed by means of a HP-3562 two-channel digital signal analyzer to characterize the preamplifier.

Fig. 2 shows the measured frequency response $A(f)$ in the frequency range 1 mHz–1 Hz for the two available roll-off frequencies. In excellent agreement with the simulation, the measured lowest roll-off frequency is 4 mHz and the gain is 80 dB $\pm$ 0.6 dB in the frequency range 20 mHz–100 kHz. The high frequency roll-off f_H = 230 kHz was evaluated by means of a swept sinusoidal generator.

The input impedance Z_{in} was measured by using the circuit of Fig. 3 where the amplifier is schematized by its equivalent two-port and V_s represents the programmable white noise source provided by the digital signal analyzer.

The input impedance can be calculated according to the following relationship:

$$Z_{in} = R_a \frac{A_z}{A - A_z} \tag{2}$$

where A_z is the frequency response V_u/V_s measured in the circuit of Fig. 3. Fig. 4 shows the magnitude of the input admittance $Y_{in} = 1/Z_{in} = G_{in}(j\omega) + j\omega C_{in}(j\omega)$ measured with R_a = 2 MΩ in the frequency range 200 Hz–100 kHz, where $G_{in} = 1/R_{in} = 1/R_1 = 10^{-8}\ \Omega^{-1}$ is negligible with respect to $\omega C_{in}(j\omega)$. It is worth noting that $\omega C_{in}(j\omega)$ is a linear function of the frequency and therefore the input impedance Z_{in} can be represented in the entire bandwidth by a R_1 = 100 MΩ resistance, and a constant capacitance of 80 pF in parallel, as schematized in Fig. 3. The measured value of C_{in} is about 30 pF larger than that predicted by simulation and measured on the input FET pair. This effect is due to the capacitance of the coaxial cable connecting the R_1–C_1 filter and the input active device, and to the parasitic capacitive coupling between the plates of C_1 (9.4 μF) and ground.

The noise characteristics of the ULNA described in this paper are schematized as usual by two equivalent input noise generators [11], [13]. The equivalent input current generator is split in two components $\sqrt{4kT\Delta f/R_{in}}$ and i_n, respectively. The first takes into account the intrinsic thermal noise of the resistor R_{in} (i.e., R_1), while the second accounts for the noise generated by the rest of the preamplifier. Both generators, together with the equivalent voltage generator e_n, are shown in Fig. 3. The power spectral density S_u of the output noise of the circuit of Fig. 3 can be evaluated by means of the following relationship:

$$S_u = |A|^2 \left[S_{en} \left| \frac{Z_{in}}{R_a + Z_{in}} \right|^2 + 4kTR_p \left| \frac{1}{1 + j\omega C_{in} R_p} \right|^2 + S_{in} |R_a // Z_{in}|^2 \right] \tag{3}$$

where $R_p = R_a // R_{in}$, S_{en} is the power spectral density of e_n, S_{in} that of i_n and the voltage and current noise generators, as well as the resistor thermal noise generators, are supposed uncorrelated. Therefore, S_{en} can be evaluated by putting $R_a = 0$ and by dividing the measured $S_u(f)$ by $|A(f)|^2$.

Instead, S_{in} can be calculated by substituting (2) in (3). After further mathematical manipulations we obtain the relationship:

$$S_{in} = \frac{S_u}{|A_z|^2 R_a^2} - \frac{S_{en}}{R_a^2} - \frac{4kT}{R_p} \tag{4}$$

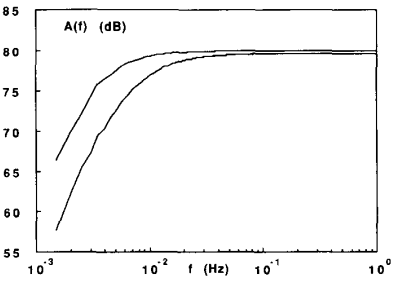

Fig. 2. ULNA measured low-frequency response for the two possible roll-off frequencies.

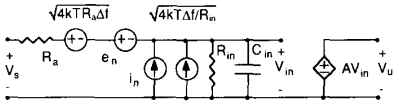

Fig. 3. Equivalent circuit representing the preamplifier and the source resistance R_a used to measure the preamplifier input impedance and equivalent noise generators. The equivalent current noise generator is splitted in two components to account for the thermal noise of R_{in} and for the rest of the circuit.

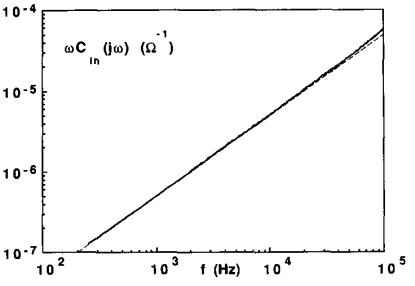

Fig. 4. Measured capacitive part $\omega C_{in}(j\omega)$ of the preamplifier input conductance Y_i. The contribution of the input resistor $G_{in} = 1/R_1$ was substracted from the measured Y_i. The almost perfect linearity with frequency allows the schematization of the input impedance with a resistance-capacitance parallel.

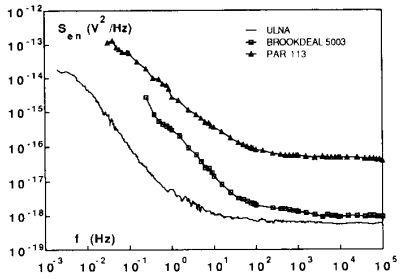

Fig. 5. Power spectral density of the equivalent input voltage noise generator of ULNA and comparison with those of commonly used commercial preamplifiers.

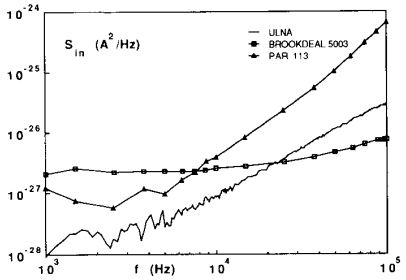

Fig. 6. Power spectral density of the equivalent input current noise generator of ULNA and comparison with those of commonly used commercial preamplifiers (the contribution due to the thermal noise of the amplifier input resistance R_{in} is subtracted).

Fig. 5 shows S_{en} in the frequency range 1 mHz – 100 kHz. S_{en} is white and equal to 0.64 nV/Hz$^{1/2}$ above 10 Hz and this plateau is mainly due to the superposition of two effects: the Johnson noise of resistor R_2 (0.4 nV/Hz$^{1/2}$) and the voltage noise of the input FET pair (0.5 nV/Hz$^{1/2}$); the residual part comes from the current generator $F2$. Fig. 6 shows S_{in} in the frequency range 1 kHz–100 kHz, where its effects are not negligible with respect to that of the Johnson noise of R_p (R_a = 10 MΩ in this measurement). At present, the physical origin and the real allocation in the circuit of the phenomenon whose effects S_{in} takes into account is not clear, but the experiments show that the schematization utilized is effective at least for R_a values as high as 10 MΩ.

Fig. 5 and 6 also show for comparison the corresponding quantities measured on two commercial low-noise preamplifiers (Brookdeal 5003 and PAR 113). The improvement obtained in S_{en} in the entire bandwidth is evident especially at low frequency, where our ULNA is better at least by a factor of 50. As far as the total output noise S_u is concerned, the comparison between ULNA and PAR 113 always results strongly favorable to our amplifier, whereas that between ULNA and Brookdeal 5003 depends on the value of the source resistance R_a and on the frequency range of the measurement. For instance, our ULNA is better in the entire bandwidth up to 100 kHz if R_a is less than 2 kΩ. In fact, the effect of S_{in} is negligible with respect to that of S_{en} in this case. For higher values of R_a, ULNA is always better below 20 kHz, because also the power spectral density of its equivalent input current noise generator is lower than that of Brookdeal 5003. This means that using our ULNA is greatly advantageous in most LFNM technique applications. In order to complete the comparison, it should be pointed out that both the above-mentioned preamplifiers are characterized by an input resistance of 100 MΩ and by an input capacitance of 15 pF, lower than that of our ULNA.

Other important parameters characterizing an amplifier operating at very low frequency are the warm-up time T_w, and the settling time T_s. T_w is the time elapsed since the power-on and the thermal regime of the equipment. T_s is the time elapsed, after T_w, since the input signal application and the time at which it is possible to begin a measurement, with the above-mentioned noise and frequency response characteristics. Tests demonstrated that this goal can be achieved when the output offset V_o enters in the range ±20 mV, after the transient caused by the application of the input signal. The measurement of V_o versus time t obtained after a warm-up time T_w = 2 h, then by putting the switch $S1$ in position 2 (fast recover) for 5 minutes and by switching it in position 1 at t = 0, is reported in Fig. 7. It shows that T_s is 230 s. During the transient the amplifier output does not saturate, the maximum V_o being less than a few hundreds of mV. Therefore, it is possible to perform noise measurements at very low frequency only a few minutes after signal application.

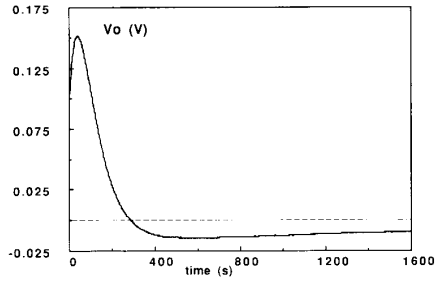

Fig. 7. Output transient measured after a warm-up time of 2 h, and a recover of 5 minutes (switches $S1$ in 2). Considering the amplifier fully operative when the output offset is within ±20 mV, the settling time is about 4 min. Note that the amplifier output is well away from saturation during the transient.

IV. Applications

The realization of an ultra low-noise amplifier with noise characteristics at low frequency better than those currently available can be particularly useful in several applications where the preamplifier intrinsic noise determines an impassable limit to the realization of a specific experiment.

The ULNA described in the above Sections was mainly used in our laboratory in noise measurements on electronic components, in particular in the detection and study of the electromigration noise in thin metal films [3], [4], and in the generation of $1/f^\gamma$ noise.

As far as noise generation is concerned, it was recently shown that $1/f^\gamma$ noise can be generated by summing a very low number of Lorentzian spectra $S_L = \tau/(1 + 4\pi^2 f^2 \tau^2)$, provided that their relaxation times τ are distributed according to the law $1/\tau^\gamma$ [14]. The hardware realization of a $1/f^\gamma$ noise generator on a frequency band of seven decades according to this principle was permitted by the low-noise characteristics and the high input impedance presented by our ULNA [15]. Each Lorentzian spectrum was generated by filtering the thermal noise of a given resistor R with a parallel capacitor C. The sum of M spectra was obtained by putting M parallels R–C in series and collecting the voltage noise generated at the ULNA input. The proper distribution of the time constants was obtained by keeping a fixed

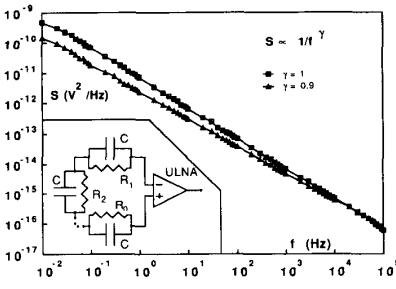

Fig. 8. Schema of the $1/f^{\gamma}$ noise generator and measured power spectral density of the generated noise, for values of the exponent γ equal to 1 and 0.9 (from [15]).

value of the capacitor C and choosing accordingly a value of R_i, in order to have $\tau_i = R_i C$. Values of R_i typically range from tens of Ohms to tens of MegaOhms. The generator schematic together with experimental results showing the generated $1/f^{\gamma}$ noise for two different exponents are shown in Fig. 8. It is worth noting that the wide band obtained is essentially due to the amplifier noise performance in the low-frequency range.

V. Conclusions

Commercial preamplifiers presently available on the market show a relatively high low-frequency limit (for instance Brookdeal 5003) and/or not excellent background noise performance in the frequency range below a few Hz (for instance PAR 113). On the other hand, there are several applications in which low-frequency noise measurements have to be extended below a few Hertz, with still-optimum noise performance. This allows the exploration of a frequency band where some physical phenomena, such as the electromigration noise, can be better investigated. It is therefore advisable to realize custom amplifiers which address this requirement, with a design dedicated to the low-noise performance and the solution of typical problems occuring at low-frequency.

The ULNA described in this work answers to these qualifications. In fact, its bandwidth extends over seven decades starting from 4 mHz and its equivalent input noise can be represented, in most applications, by the equivalent voltage noise generator of the less noisy active device available on the market: the FET 2SK146. This means that the corner frequency of the power spectral density of the input noise voltage generator is about 3 Hz, with a white noise plateau equal to the Johnson noise of a 35-Ω resistor.

This performance allowed, for instance, the realization of a standard $1/f^{\gamma}$ noise generator operating over seven decades, and the extension of the analysis of the noise phenomena in electronic devices and materials to a frequency limit about two orders of magnitude lower than that allowed by previously available instrumentation.

The scheme of the ULNA is very simple and the cost of its realization can be roughly estimated at least an order of magnitude less than that of a commercial preamplifier, whereas its reliability has been widely tested during more than three years of use in our laboratories. For these reasons, we believe that many experimenters operating in the field of low-frequency noise measurements could take advantage by its utilization, in order to perform experiments at low frequency with very good noise performance, at present not available with commercial laboratory instruments.

References

[1a] See, for example, in the series *Proc. Int. Confs. on Noise in Physical Systems and 1/f Noise:* P. H. E. Meijer, R. D. Mountain, and R. J. Soulen, Eds., *Proc. 6th Int. Conf. on Noise in Physical Systems*. Washington, DC, 1981.

[1b] See, for example, M. Savelli, G. Lecoy, and J. P. Nougier, Eds., *Noise in Physical Systems and 1/f Noise*. Amsterdam, The Netherlands: Elsevier Science, 1983.

[1c] See, for example, A. D'Amico and P. Mazzetti, Eds., *Noise in Physical Systems and 1/f Noise*. Amsterdam, The Netherlands: Elsevier Science, 1986.

[1d] See, for example, C. M. Van Vliet, Ed., *Noise in Physical Systems*. Singapore: World Scientific, 1987.

[1e] See, for example, A. Ambrózy, Ed., *Noise in Physical Systems*. Budapest, Hungary: Akadémiai Kiadó, 1990.

[2] M. Celasco and F. Fiorillo, "Current noise measurements in continuous metal thin films," *Appl. Phys. Lett.*, vol. 26, pp. 211–212, 1975.

[3] B. Neri, A. Diligenti, and P. E. Bagnoli, "Electromigration and low-frequency resistance fluctuations in aluminum thin-film interconnections," *IEEE Trans. Electron Devices*, vol. ED-34, pp. 2317–2321, 1987.

[4] A. Diligenti, P. E. Bagnoli, B. Neri, S. Bea, and L. Mantellassi, "A study of electromigration in aluminum and aluminum-silicon thin-film resistors using noise technique," *Solid State Electron.*, vol. 32, pp. 11–16, 1989.

[5] J. G. Cottle, and T. M. Chen, "Activation energies associated with current noise of thin metal films," *J. Electron. Mat.*, vol. 17, pp. 467–471, 1988.

[6] B. Pellegrini, R. Saletti, P. Terreni, and M. Prudenziati, "$1/f^{\gamma}$ noise in thick-film resistors as an effect of tunnel and thermally activated emissions, from measures versus frequency and temperature," *Phys. Rev. B*, vol. 27, pp. 1233–1243, 1983.

[7] M. J. Kirton and M. J. Uren, "Noise in solid-state microstructures: A new perspective on individual defects, interface states and low-frequency ($1/f$) noise," *Adv. Phys.*, vol. 38, pp. 367–468, 1989.

[8] M. A. Caloyannides, "Microcycle spectral estimates of $1/f$ noise in semiconductors," *J. Appl. Phys.*, vol. 45, pp. 307–316, 1974.

[9] G. V. Pallottino and G. Vannaroni, "A low-noise low-input conductance preamplifier for gravitational research," *IEEE Trans. Instrum. Meas.*, vol. IM-34, pp. 676–680, 1985.

[10] R. B. Hallgren, "Paralleled transconductance ultralow-noise preamplifier," *Rev. Sci. Instrum.*, vol. 59, pp. 2070–2074, 1988.

[11] Y. Netzer, "The design of low-noise amplifiers," *Proc. IEEE*, vol. 69, pp. 728–741, 1981.

[12] B. Pellegrini, R. Saletti, B. Neri, and P. Terreni, "Minimization of low-frequency noise sources in electronic measurements," in *Noise in Electrical Measurements, Proc. 1st Int. Symp. on Measurement of Electrical Quantities*, pp. 195–200, IMEKO, Budapest 1985.

[13] C. D. Motchenbacher and F. C. Fitchen, *Low Noise Electronic Design*. New York: Wiley, 1973.

[14] B. Pellegrini, R. Saletti, and B. Neri, "Minimum number of Lorentzian spectra sufficient to give $1/f^{\gamma}$ spectrum," *Alta Frequenza*, vol. 55, pp. 245–253, 1986.

[15] B. Pellegrini, R. Saletti, B. Neri, and P. Terreni, "$1/f^{\gamma}$ noise generators," in *Noise in Physical System and 1/f Noise*, A. D'Amico and P. Mazzetti, Eds. Amsterdam, The Netherlands: Elsevier, 1986, pp. 425–428.